CALCULATION OF PARAMETERS OF HEAT PIPE WITH CONVECTIVE HEAT TRANSFER

V. F. Frolov, E. M. Vernikov, and É. S. Savkov

UDC 66.045

A method of calculating a heat pipe with due allowance for the rate of heat transfer on the boundary is given. The theoretical data are compared with experimental results.

The scale and areas of application of heat pipes (HP) in contemporary technology are now being expanded [1]. Heat pipes function as an intermediate heat carrier in various devices and are of diverse designs. Yet the available studies (T. Cotter et al.) do not satisfy the demands of practice, since they do not allow a simultaneous and equal consideration of the heat transfer due to the internal mechanism of HP and the rate of heat transfer from outside for all its zones [2, 3]. In many interesting cases of application of HP, e.g., in chemical technology, air-conditioning systems, etc., the evaporator and condenser sections exchange heat by convection with the surroundings. The distribution of the density of heat flux through the wall along the sections is determined, other conditions being equal, by its temperature field. For HP with evaporator and condenser sections of large area and high vapor flow velocities, close to sonic, the nature of the distribution of the density of the heat flux normal to the wall over the length has a significant effect on the axial heat load.

The evaporator section of a HP with a prescribed density distribution of heat flux through the wall was calculated in [4].

In the present paper we describe a method of calculating an HP as a whole, with emphasis on the conditions of heat transfer with the surroundings, whereas the thermal resistance of the wick is assumed to be known or can be calculated by known methods. The method can be used for heat calculations for devices in which the HP acts as an intermediate heat carrier, A common feature of such devices is that their evaporator and condenser sections are in a flow of medium at different temperatures.

For an HP with prescribed design characteristics and a prescribed heat-transfer law at its surface the presented method can be used to determine the axial heat load, the density distribution of the heat flux through the wall, the temperature distribution on the liquid–vapor interface and the outer wall surface. We can also solve the inverse problem, i.e., select design characteristics for an HP from prescribed values of regime parameters.

The mathematical model is formulated for steady-state heat and mass transfer in the HP. We assume that the vapor in the HP obeys the Clapeyron equation of state and the Euler equation of motion

$$p = \rho RT, \tag{1}$$

$$w\frac{dw}{dz} = -\frac{1}{\rho}\operatorname{grad} p. \tag{2}$$

In addition, the vapor is on the saturation line and is characterized by the integral of the Clausius–Clapeyron equation

$$\frac{p}{p_a} = \exp\left[\frac{L}{R}\left(\frac{1}{T_a} - \frac{1}{T}\right)\right]. \tag{3}$$

The constant of integration was determined from the condition for the adiabatic section.

Lensovet Leningrad Technological Institute. Translated from Inzhenerno-Fizicheskii Zhurnal, Vol. 38, No. 2, pp. 222-230, February, 1980. Original article submitted January 11, 1979.

 0022-0841/80/3802-0132$07.50 © 1980 Plenum Publishing Corporation

The vapor flow in the HP is assumed to be one-dimensional with injection or withdrawal of mass through the wall of the corresponding section. The continuity equation can then be written in the form

$$\frac{d}{dz}(\rho w) = \frac{\Pi q}{AL}. \tag{4}$$

The heat flux density on the liquid–vapor interface for evaporation and condensation is determined from the equation

$$q = \varphi(\beta)\frac{L\Delta p}{\sqrt{2\pi RT}}, \quad \varphi(\beta) = \frac{\beta}{1 - 0.4\beta}, \tag{5}$$

where Δp is the difference between the saturated vapor pressure in the HP and the saturated vapor pressure at the temperature of the phase interface. The function $\varphi(\beta)$ takes into account [5] the effect of macroscopic flow of vapor normal to the phase interface on evaporation and condensation.

Heat transfer through the wall and through the wick, filled with working fluid, is effected by conduction. Assuming that the thickness of the wall and wick is small in comparison with the diameter of the vapor channel, we obtain for the density of the heat flux through the wall

$$q = \lambda\frac{T_w - T_l}{\delta}, \tag{6}$$

where δ is the total thickness of the wall and wick; λ is the effective thermal conductivity of the wall and wick, given by the equation for a layered wall

$$\frac{\delta}{\lambda} = \sum_{i=1}^{n}\frac{\delta_i}{\lambda_i}.$$

The layers of the wall here are the HP container wall, the fluid-filled wick, and the liquid film on the wick surface in the condenser.

We neglect heat transfer by conduction in the direction of the vapor flow. We assume that heat transfer along the HP is due entirely to phase transitions and hydrodynamic factors.

The indicated system of equations is closed if either the temperature of the wall outer surface (boundary conditions of first kind), or the density of the heat flux through the wall (boundary conditions of second kind), is prescribed.

We assume in what follows that the zero of the z axis coincides with the start of the evaporator and condenser sections, and its direction is the same as that of the vapor flow. As the positive direction of the heat flux normal to the wall we take its direction in the condenser section.

Using Eqs. (1), (2), and (3), performing some algebra, and integrating in the limits $\bar{w} - 1$ and $\bar{p} - 1$, we obtain

$$\bar{w}^2 = 1 + K_2\ln(1 - K_1\ln\bar{p}), \tag{7}$$

where K_1 and K_2 are dimensionless complexes:

$$K_1 = \frac{R}{L}T_a, \quad K_2 = 2L^3\left(\frac{A}{R}\right)^2\left(\frac{p_a}{QT_a}\right)^2.$$

On conversion to dimensionless quantities here and henceforth we use the values of the corresponding quantities for the adiabatic section as scales.

Equation (4) after integration can be put in the form

$$\frac{\bar{p}\bar{w}}{\bar{T}} = \int_0^{\bar{z}}\bar{q}(\eta)\,d\eta. \tag{8}$$

Substituting in (8) the expressions for the velocity from (7) and the temperature from (3) we obtain the first theoretical equation

$$\delta_{ij} - \bar{p}(1 - K_1 \ln \bar{p})[1 + K_2 \ln (1 - K_1 \ln \bar{p})]^{\frac{1}{2}} = \int_0^{\bar{z}} \bar{q} d\eta, \tag{9}$$

where

$$\delta_{ij} = \begin{cases} 0, & i \neq j \quad \text{(for the evaporator)}, \\ 1, & i = j \quad \text{(for the condenser)}. \end{cases}$$

The second theoretical equation is Eq. (5) converted to

$$\bar{q}\sqrt{\overline{T_l}} = K_3\left[\bar{p} - \exp\left(\frac{1}{K_1}\left(1 - \frac{1}{\overline{T_l}}\right)\right)\right], \qquad K_3 = \varphi(\beta)\, lL\sqrt{\frac{\overline{2A}}{R}}\,\frac{p_a}{Q\sqrt{T_a}}. \tag{10}$$

We obtain the other two equations, using (6) and the boundary condition corresponding to convective heat transfer when the thickness of the wall and wick is small:

$$\lambda\frac{T_w - T_l}{\delta} = \alpha(T_w - T_f)$$

When T_f = const and α = const,

$$\bar{T}_l = \bar{T}_f + K_4\bar{q}, \quad \bar{T}_w = \bar{T}_f + K_5\bar{q}, \qquad K_4 = \frac{1}{A_w}\left(\frac{\delta}{\lambda} + \frac{1}{\alpha}\right)\frac{Q}{T_a}, \quad K_5 = \frac{1}{\alpha A_w}\,\frac{Q}{T_a}. \tag{11}$$

Neglect of viscosity effects in the vapor flux in the adopted theoretical equations (9)-(11) is valid for the limiting case of predominant effect of change in momentum, which is the case at high radial Re. From a comparison of theoretical and experimental results [6] we can affirm that the model of an ideal gas and real vapor phase in the HP is satisfactory when the ratio of the vapor velocity normal to the phase interface and the axial velocity lies in the range 0.005-0.03.

The theoretical equations are valid for the temperature range corresponding to subcritical modes of operation of the HP (gasdynamic blocking of vapor channel, overdrying of wick). Combination of the design characteristics, thermophysical properties, and kinetic data in dimensionless complexes enables us to use the theoretical results for all HP for which the respective complexes are equal.

The complex K_1 contains only the thermophysical properties of the working fluid and the temperature of the adiabatic section and, hence, is common to the evaporator and condenser sections. The other complexes for the heated and cooled sections may differ in the numerical value of the heat-exchange surface, heat-transfer coefficient, etc.

Equations (9)-(11) are valid for systems in which the heat agents flowing over the evaporator and condenser sections have a uniform temperature, due to intensive mixing, for example. If the section is in a flow of mixture whose temperature varies in the direction of vapor flow owing to heat exchange with the wall we can use an additional equation, which for a coolant has the form

$$\bar{T}_x = \bar{T}_{x0} + K_6\int_0^{\bar{z}} \bar{q} d\eta, \quad K_6 = \frac{1}{c_{px}G}\,\frac{Q}{T_a}. \tag{12}$$

In addition, Eqs. (9)-(11) are written for second-generation HP, in which the condensate flows into the evaporator section through special capillary arteries situated in the region of the vapor channel [7]. In such devices the thickness of the liquid layer in the wick depends on the HP load. In first-generation HP all the condensate flows into the evaporator

through the capillary system contiguous with the wall. Hence, the theoretical equations will have to take into account the variation of the thermal resistance of the wick with HP load, for which we use the formula for the thickness of the layer of liquid filling the wick

$$\delta = \frac{\mu_l Q}{\rho_l L x_w \Pi \left(\frac{2\sigma}{r_{cap} l_{eff}} + \rho_l g \right)}, \quad l_{eff} = l_a + \frac{l_e + l_c}{2}. \tag{13}$$

Formula (13) was obtained with the aid of the D'Arcy equation; the expression in parentheses gives the pressure drop in the wick due to the action of capillary and gravitational forces. Substituting (13) for the thickness of the liquid layer in complex K_4, we obtain a formula that takes into account its variation with HP load in a more complex manner.

Equations (9)-(11) were solved numerically by computer. For calculation of the evaporator or condenser sections the prescribed parameter can be the temperature of the adiabatic section T_a or the axial heat flux Q, which are fixed in the calculation.

We consider the calculation procedure with a prescribed HP load. In a first approximation the dimensionless complexes K_i are calculated for a tentatively selected temperature of the adiabatic section. Equation (9) is solved for a specified axial coordinate and an approximately prescribed density of heat flux through the wall. For the same coordinate Eq. (10) is then solved for $\bar{q}$ for a pressure value previously calculated from (9). Equations (9) and (10) are solved in turn until the relative difference between the two successive approximations of $\bar{q}$ becomes sufficiently small.

After the whole heat-transfer section (evaporator or condenser) has been traversed an assessment of the fulfillment of the integral equality

$$\int_0^1 |\bar{q}(\eta)| \, d\eta = 1 \tag{14}$$

is made. If the calculated value of the integral for the evaporator is less than unity the next cycle of calculations from (9)-(10) is carried out for a lower temperature of the adiabatic section. For the condenser the inverse relation must be satisfied. The solution of (9) and (10) for different T_a is continued until a value of the temperature of the adiabatic section corresponding to fulfillment of equality (14) with prescribed accuracy is selected. The HP load in the case of a prescribed temperature of the adiabatic section is determined in a similar way.

For joint calculation of the evaporator and condenser sections, i.e., for calculation of the HP as a whole, both the HP load and the temperature of the adiabatic section have to be selected. Hence, for combined calculation of the HP sections fulfillment of equality (14) in the evaporator is obtained by a change in T_a, and then fulfillment of equality (14) in the condenser (with T_a obtained by calculation) is obtained by a choice of Q, which is also contained in the dimensionless complexes. We then proceed again to the evaporator, using the calculated value of Q, and so to satisfaction of equality (14) with prescribed accuracy.

The results of the complete calculation of an HP from the presented procedure for an HP filled with acetone are shown in Fig. 1. Equations (12) and (13) were also used in the calculation. This figure shows the experimental values of the HP heat load and the temperature of the adiabatic section. The experiments were conducted on a cylindrical HP 0.5 m long with a vapor channel 8 mm in diameter. The wick was a bulky metal screen. The evaporator section was immersed in a temperature-controlled mixed liquid, and the condenser was cooled with flowing liquid in a double pipe heat exchanger. As Fig. 1 indicates, the agreement of the experimental and calculated values is satisfactory.

One way of increasing the output of plasmachemical technology is improvement in heat recuperation systems [8]. The problem consists, in particular, in the heating to high temperature of the agent cooling the reaction products. The problem can be solved by an increase in the surface in contact with the coolant and a reduction in the temperature drop when the heat is transferred from the high-temperature zone occupied by the reaction products. Of known devices heat pipes are best able to satisfy such requirements.

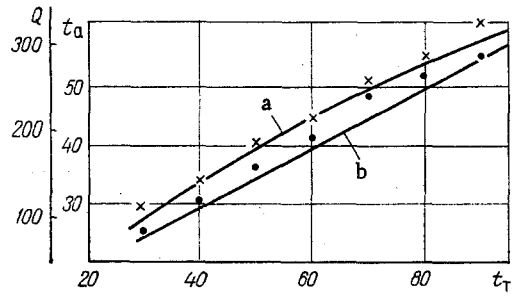

Fig. 1

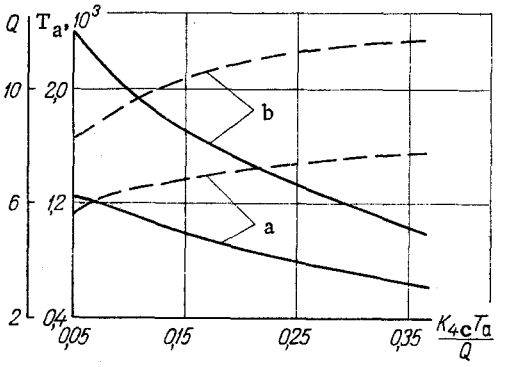

Fig. 2

Fig. 1. Load Q (W) of heat pipe (a) and temperature t_a (°C) of adiabatic section (b) as function of temperature t_T of outer medium flowing over the evaporator section (the points are the measured values; the curves are the calculated values); $K_{1e} = K_{1c} = 2.7 \cdot 10^4 T_a$; $K_{2e} = K_{2c} = 3.7 \cdot 10^6 (p_a/QT_a)^2$; $K_{3e} = 0.53 p_a/Q\sqrt{T_a}$; $K_{3c} = 0.77K_{3e}$; $K_{4e} = 3.4 \cdot 10^{-4} Q^2/T_a$; $K_{4c} = 0.73K_{4e}$; $K_{6c} = 0.01Q/T_a$.

Fig. 2. Calculated dependences of heat flux power Q, kW (continuous curves); drawn off from reaction products with temperature $T_T = 2000$°K (a) and 3000°K (b), and of temperature of vapor in adiabatic section T_a, °K (dashed curves), on complex of design and kinetic parameters of heat-pipe condenser section. The working fluid was sodium, the initial temperature of the coolant was 300°K; $K_1 = 8.6 \cdot 10^{-5} T_a$; $K_2 = 3.7 \cdot 10^6 (p_a/QT_a)^2$; $K_{3e} = 0.53 p_a/(Q\sqrt{T_a})$; $K_{3c} = 10K_{3e}$; $K_{4e} = 0.1Q/T_a$; $K_{6c} = 0.1 \cdot Q/T_a$.

Figure 2 can be used to estimate the range of temperature in which practical realization of a specific HP is possible. With its help we can also select condenser design parameters and kinetic coefficients for which heat recuperation is feasible.

The nature of the distribution of some quantities along the condenser is illustrated in Fig. 3. In the case of a symmetric HP, i.e., one in which the evaporator and condenser have the same geometric dimensions and the kinetic coefficients are equal, the presented curves are symmetric relative to the adiabatic section (within the framework of the adopted ideal-gas model) for the vapor phase. However, the temperature drops between the adiabatic section and the external heat carrier, on the one hand, and the external coolant, on the other, generally differ in absolute value. For instance, for the regime corresponding to the data of Fig. 3, we can obtain the following estimate:

$$\frac{|T_a - T_T|}{T_a - T_x|} = \frac{|253.5 - 400|}{|253.5 - 119|} = 1.09.$$

The difference in temperature drops can probably be attributed to asymmetry of the function for the vapor mass flux density for evaporation and condensation relative to zero.

Equation (9) takes into account the effect of pressure distribution in the vapor phase on the heat flux density along the HP. If the change in vapor pressure along the HP is small, Eq. (9) can be neglected in the calculation. The practical difficulty of calculation lies in the fact that in this equation the complexes K_1 and K_2 contain the regime parameter T_a, which can be determined.

The pressure drop in the vapor phase in the sonic regime can be estimated with the aid of the graphic relations in Fig. 4, which shows the pressure distribution in the evaporator for monatomic, diatomic, and polyatomic molecules, and also the velocity of the vapor relative to the velocity of sound, and its density. As the figure indicates, the maximum pressure drop increases with reduction in the number of atoms in the molecule.

The presented curves were obtained with the aid of the same initial equations as system (9)-(11). The relation between M, $\bar{q}$ and $\bar{z}$ was obtained on the assumption of constancy of the velocity of sound along the HP:

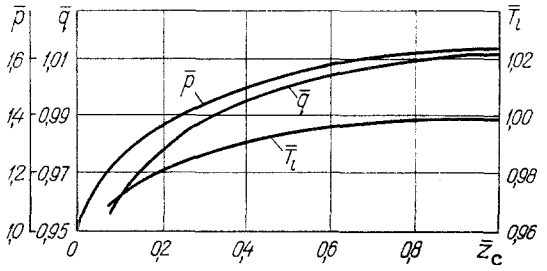

Fig. 3

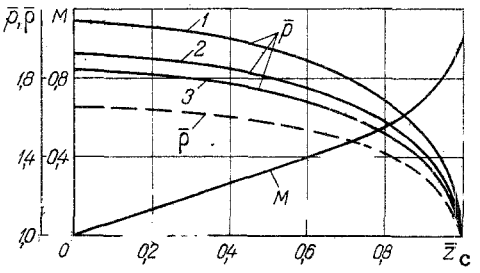

Fig. 4

Fig. 3. Distribution of relative pressure, density of heat flux through wall, and phase interface temperature along condenser section in sonic regime with uniform ambient temperature: $K_1 = 0.07$; $K_2 = 29.18$; $K_3 = 1.6$; $K_4 = 0.53$; $T_a = 253.5°K$; $T_T = 400$; $T_X = 119°K$.

Fig. 4. Distribution of relative vapor pressures p for monatomic, diatomic, and polyatomic molecules, density ρ, and velocity of vapor flow M for constant density of heat flux through the evaporator wall: 1) $\varkappa = 1.67$; 2) 1.41; 3) 1.29.

$$M = C_1 \exp\left[\int \left(\bar{q}\, d\bar{z} \Big/ \int_0^{\bar{z}} \bar{q} d\eta\right) + \frac{M^2}{2}\right],$$

where C_1 is a constant of integration. The relation between $\bar{p}$ and M contains the assumption of constancy of the vapor temperature over the length:

$$\bar{p} = 1 - \frac{c_p}{c_v}\left[1 - \exp\left(\frac{M_a^2 - M^2}{2}\right)\right].$$

As the comparison shows, the maximum pressure drops in the vapor phase along the HP sections, according to the data in Fig. 4, are ≈15% higher than those given by Eq. (9), but below those given in [9], where the relative pressure drops were estimated with the aid of the law of conservation of momentum for a vapor of constant density.

We note in conclusion that the presented method can be used both for calculations of the parameters of existing HP, containing a wick of known thermal resistance, in new operating conditions, and for the development of new designs. It is assumed in the latter case that the thermal resistance of the wick can be determined by known methods, and the effect of HP load and physical properties of the working fluid on the thickness of the condensate layer in the capillaries near the wall is given by Eq. (13), for instance.

NOTATION

R, L, gas constant and heat of vaporization of working fluid; g, gravitational acceleration; ρ_l, μ_l, density and dynamic viscosity of working fluid in wick; σ, coefficient of surface tension of working fluid; c_{pc}, G, heat capacity and mass flow of external coolant flowing over condenser; $\varphi(\beta)$, known function of condensation coefficient β; A_w, α, heat-exchange surface and heat-transfer coefficient outside evaporator or condenser; δ, λ, total thickness and effective thermal conductivity of wall and fluid-filled wick; $\varkappa_w$, permeability of wick; Q, heat pipe load (axial heat flux); q, density of heat flux through wall of evaporator or condenser; l, length of evaporator or condenser section; Π, A, perimeter and cross-sectional area of vapor channel; r_{cap}, effective radius of wick capillary; T, p, temperature and pressure (of vapor); ρ, w, density and axial velocity of vapor; a, velocity of sound in vapor; c_p, c_v, heat capacity at constant pressure and volume. Subscripts: a, e, c, adiabatic, evaporator, and condenser sections, respectively; l, liquid–vapor interface; w, external heat-exchange surface of evaporator or condenser; f, external medium flowing over sections of heat pipe; τ, heat carrier; x, coolant; x0, initial temperature of coolant; $\bar{z} = z/l$; $\bar{T} = T/T_a$; $\bar{p} = p/p_a$; $\bar{\rho} = \rho/\rho_a$; $\bar{T}_l = T_l/T_a$; $\bar{T}_w = T_w/T_a$; $\bar{T}_f = T_f/T_a$; $\bar{q} = ql\Pi/Q$; $M = w/a$; $\varkappa = c_p/c_v$,

LITERATURE CITED

1. L. L. Vasil'ev, Inzh.-Fiz. Zh., 31, No. 5 (1976).
2. Z. R. Gorbis, in: Heat and Mass Transfer [in Russian], Vol. 10, Nauka i Tekhnika, Minsk (1973), p. 577.
3. V. Ya. Sasin, in: Heat and Mass Transfer [in Russian], Vol. 10, Nauka i Tekhnika, Minsk (1973), p. 578.
4. E. M. Vernikov, V. F. Frolov, and P. G. Romankov, Zh. Prikl. Khim., 48, No. 9 (1975).
5. D. A. Labuntsov, Teplofiz. Vys. Temp., 5, No. 4 (1967).
6. G. A. Carlson and M. A. Hoffman, in: Heat Pipes [Russian translation], Mir, Moscow (1972).
7. M. Groll and P. Zimmerman, Wärme und Stoffübertragung, 4, 5 (1971).
8. I. Pollo, Przem. Chem., 51, No. 4 (1972).
9. A. Kemme, in: Heat Pipes [Russian translation], Mir, Moscow (1972).

TURBULENT FLOW OF AQUEOUS SOLUTIONS OF MICELLE-FORMING SURFACE-ACTIVE SUBSTANCES IN GAPS BETWEEN COAXIAL CYLINDERS

A. P. Simonenko

UDC 532.517.4:532.13

The results of experimental investigations of turbulent friction reduction by additives in a gap between coaxial cylinders are given.

Some micelle-forming surface-active substances (SAS), as well as high polymers, are able to reduce the frictional drag of fluids. There have been a number of studies of turbulent drag reduction by SAS additives in tubes [1, 2]. A correlation between the onset of drag reduction and the micellar nature of SAS has been established [3], and the feasibility of using them for reduction of drag in homogeneous and suspension-laden flows has been demonstrated [4]. Several questions connected with the use of SAS additives for reduction of turbulent friction, however, are still unresolved.

In the present work we investigated the drag torque in relation to Reynolds number for flows of aqueous solutions of Ditalan OTS and Metaupon in the gap between coaxial cylinders, i.e., in conditions in which a particular friction stress can be maintained at the wall over a long period.

The experimental investigations were made on an apparatus consisting of a stainless steel cup within which three cylinders were fitted coaxially with the cup at a distance of 1 mm from one another. The upper and lower cylinders were kept stationary to eliminate end effects. The middle cylinder could rotate through 120°, and the torque developed on it due to rotation of the outer cylinder was transmitted to a force gauge, from the readings of which the drag torque was calculated from the equation

$$C_m = \frac{\tau}{\rho U^2} = \frac{M}{\rho\omega^2} \frac{1}{2\pi R^4 H}.$$

The Reynolds number was determined from the equation

$$\mathrm{Re} = U\delta/\nu = \omega R\delta/\nu.$$

Figure 1 shows the drag torque as a function of Re for an aqueous 1% solution of Ditalan OTS containing different concentrations of sodium chloride.

Research on the effect of additions of electrolytes on the hydrodynamic effectiveness of SAS solutions is of great interest, since it is known that their presence greatly reduces the concentrations of SAS at which spherical and anisometric structures composed of individual SAS molecules (ions) are formed. The Reynolds number was calculated from the viscosity

Donetsk State University. Translated from Inzhenerno-Fizicheskii Zhurnal, Vol. 38, No. 2, pp. 231-234, February, 1980. Original article submitted January 29, 1979.

 0022-0841/80/3802-0138$07.50 © 1980 Plenum Publishing Corporation